

TECHNIQUES FOR PHYSIOLOGY

In vivo Ca²⁺ imaging of dorsal horn neuronal populations in mouse spinal cord

Helge C. Johannssen and Fritjof Helmchen

Department of Neurophysiology, Brain Research Institute, University of Zurich, Zurich, Switzerland

Two-photon Ca²⁺ imaging allows functional studies of neuronal populations in the intact brain, but its application to the spinal cord *in vivo* has been limited. Here we present experimental procedures to label superficial dorsal horn populations with Ca²⁺ indicator and to stabilize the spinal cord sufficiently to permit functional imaging in anaesthetized mice. Spontaneous Ca²⁺ transients occurred in a small subpopulation of dorsal horn cells. Larger numbers of cells were activated by increasing electrical stimulation of primary afferent fibres. Notably, in a subset of cells we resolved Ca²⁺ transients evoked by mechanical stimulation of the paw. These advances open new opportunities to study both physiology and pathology of spinal cord neural circuits *in vivo*.

(Received 20 April 2010; accepted after revision 23 July 2010; first published online 26 July 2010)

Corresponding author F. Helmchen: Brain Research Institute, University of Zurich, 8057 Zurich, Switzerland.

Email: helmchen@hifo.uzh.ch

Abbreviations OGB-1 AM, Oregon Green 488 BAPTA-1 acetoxymethyl; SC, spinal cord; SDH, superficial dorsal horn; SR101, sulforhodamine 101.

Introduction

The superficial dorsal horn (SDH) of the spinal cord (SC) is the first centrally located part of the somatosensory pathway. The SDH neuronal circuitry is essential for pre-processing peripheral inputs and relaying them to higher CNS centres involved in somatosensory coding (Willis, 2007). In particular, noxious mechanical and thermal inputs carried by C- and A δ -fibres evoke activation of SDH neuronal networks. How exactly these afferent inputs are processed by SC neuronal populations remains unclear. To further understand the physiological properties of SC circuits as well as their alterations during pathologies such as neuropathic pain, novel methods are needed to obtain a more detailed view of SDH activity patterns associated with somatosensation *in vivo*.

While patch clamp recordings allow sampling of single SC cells (Graham *et al.* 2004), recent advances in two-photon Ca²⁺ imaging, in particular bulk loading of synthetic Ca²⁺ indicators into neuronal tissue (Stosiek *et al.* 2003), have enabled optical recordings from neuronal populations with cellular resolution in living animals (reviewed in Grewe & Helmchen, 2009). *In vivo* two-photon Ca²⁺ imaging has been applied for example to monitor activity in developing SC networks in zebrafish larvae (Brustein *et al.* 2003). While similar studies have been performed in various parts of the mammalian brain,

population Ca²⁺ imaging in the SC of mice or rats has been hampered by mechanical instability. *In vivo* activity in the SDH has been visualized mostly using techniques without cellular resolution like intrinsic optical imaging (Sasaki *et al.* 2002). Only one group has so far reported [Ca²⁺]_i elevations in lamina I neurons of SDH in living rats on a minutes time scale during repetitive nerve stimulation, following subcutaneous capsaicin injection (Ikeda *et al.* 2006), and after opioid application (Drdla *et al.* 2009). Despite the significant role of SDH circuits in mechanisms of acute and chronic forms of pain, *in vivo* optical studies have thus remained scarce and rather coarse. Here we aimed at establishing *in vivo* two-photon Ca²⁺ imaging in the SDH to reveal neuronal activity patterns on the subseconds time scale. Our approach is likely to promote detailed future studies of normal and pathological population dynamics in dorsal horn neural circuits.

Methods

Animals and surgical procedures

Animal procedures were in accordance with the University of Zurich Centre for Laboratory Animals guidelines and approved by the Cantonal Veterinary Office. C57BL6-mice (2–4 months) of either sex were anaesthetised by I.P.

injection of 1.2–1.8 g kg⁻¹ urethane (Sigma, Buchs, Switzerland) supplemented with 1–2% isoflurane (Baxter, Volketswil, Switzerland) in air if needed. Depth of anaesthesia was assessed by testing corneal, ear pinch and pedal reflexes, and by monitoring breathing rate and whisker movements. Body temperature was maintained at 37°C with a heating blanket.

A dorsal laminectomy was performed at spinal levels L2–L4 (Fig. 1A). In brief, the skin was incised longitudinally and paravertebral muscles deflected to expose the vertebral column. Spinous processes and dorsal aspects of vertebral laminae were removed with a Friedman–Pearson's rongeur and the dura mater carefully opened using a 30G needle. Custom-made clamps were attached to the vertebral column rostral and caudal to the laminectomy to stabilise the preparation (Steffens *et al.* 2009). The trunk was slightly elevated and the front teeth fixed by a tooth bar (Davalos *et al.* 2008). Regular blood flow through the central posterior vessel was monitored to assess tissue health and integrity. Skin flaps and agar were used for building a reservoir of warm (37°C) normal rat Ringer solution (in mM: 135 NaCl, 5.4 KCl, 5 Hepes, 1.8 CaCl₂, pH 7.2) to allow use of immersion objectives and to prevent drying out of the SC. Warm Ringer solution was repeatedly applied throughout the experiment. A small slit was made in the pia to allow penetration of a pipette for dye injection. For staining and imaging the mouse was rotated around the longitudinal axis by about 40 deg (Fig. 1B) to obtain a nearly perpendicular pial surface and thereby optimize optical access to the lumbar grey matter. At the end of the experiment, the animals were killed by an overdose of anaesthetic.

Staining procedures and two-photon microscopy

For multi-cell bolus loading of Ca²⁺ indicator (Stosiek *et al.* 2003), the acetoxymethyl (AM) ester form of Oregon Green 488 BAPTA-1 (OGB-1 AM; Invitrogen, Basel, Switzerland) was dissolved in DMSO plus 20% Pluronic F-127 and diluted in Ringer solution to a concentration of 1 mM. Small amounts of a red fluorescent dye were added for pipette visualization, either Alexa Fluor 594 or sulforhodamine 101 (SR101) (both from Invitrogen), which in the neocortex specifically labels astrocytes (Nimmerjahn *et al.* 2004). In some experiments, the fixable SR101 analogue Texas Red hydrazide (TRH; Invitrogen) was added to the spinal surface and the animal perfused after *in vivo* imaging for immunohistochemical stainings (see Supplementary Methods and Supplementary Fig. 1). After dye-filling, the tip of the micropipette was first positioned above the SDH grey matter under video guidance using an Olympus 10× air objective (NA 0.3, Melville, NY, USA). The pipette was then inserted from the lateral side through the pial opening at about 500 μm lateral from the midline in

two-photon imaging mode and advanced approximately 200 μm. Dye was pressure-ejected (150–700 mbar) at about 100–200 μm depth for several minutes. To stabilise the SC for functional *in vivo* imaging the laminectomy was covered with agarose (type III-A, Sigma; 1% in Ringer solution) and a coverglass (Fig. 2A). Ca²⁺ imaging was started about 45 min after dye injection. Fluorescence signals were measured at a frame scanning rate of 4–8 Hz (128 × 128 pixel images) with a custom-built two-photon microscope using a Ti:sapphire laser (Maitai, Newport-Spectra Physics, Darmstadt, Germany) tuned to 870 nm wavelength and a 40× immersion objective (NA 0.8, Olympus). Laser power was adjusted depending on the imaging depth (maximally up to several hundred milliwatts at the objective's back aperture). Movies were imported into ImageJ (version 1.42, NIH, USA, <http://rsbweb.nih.gov/ij/>) and fluorescence traces were analysed from somatic regions of interest and expressed as relative percentage changes ($\Delta F/F$) after background subtraction. Analysis routines were written in IgorPro software (WaveMetrics, Lake Oswego, OR, USA). Data are given as means ± S.E.M.

Stimulation protocols

Primary afferent fibres were electrically stimulated with a glass electrode inserted into a fibre bundle proximal to the labelled region. Stimulation consisted of either single 50 μs pulses or trains of 10 pulses (0.5 ms length) at 50 Hz. Stimulus intensities ranged from 10 to 500 μA. For noxious mechanical stimulation, the ipsilateral hindpaw was repeatedly pinched (about 200 ms stimulus duration) using a pressure-driven serrated forceps (Graham *et al.* 2004).

Results

Ca²⁺ indicator labelling and imaging in the SC

We exposed the mouse SC by dorsal laminectomy at spinal levels L2–L4 for multicell bolus loading of Ca²⁺ indicator and *in vivo* two-photon imaging (Fig. 1A and B; see Methods). Using the dorsal SC vasculature as landmarks, OGB-1 was injected into SDH grey matter about 200–400 μm lateral from the midline, yielding robust staining of neuronal and glial cell populations (Fig. 1C). In the medial part the vast majority of labelled cells was found near the surface, displayed relatively high levels of baseline fluorescence and had typical glial morphology such as ramified processes and contact with blood vessels (Fig. 1C). In contrast, weakly stained cells were preferentially found more laterally in the superficial grey matter (Fig. 1C) likely representing a neuronal phenotype. Usually some bright OGB-1-labelled cells (23.5 ± 1.1%; *n* = 7) were interspersed among these grey matter cell populations, presumably representing glial

cells. Although attempts to counterstain glial cells with SR101 or a fixable analogue (Nimmerjahn *et al.* 2004) did result in staining of similar interspersed cells, we also found some overlap with neuronal markers so that the specificity of SR101 staining remained inconclusive (Supplementary Fig. 1, see also Discussion). A single OGB-1 injection stained hundreds of SDH cells within a tissue volume of several 100 μm diameter similar to bulk loading in neocortex (Stosiek *et al.* 2003). Cells could be resolved down to a maximum imaging depth of about 200 μm , corresponding to the first two SC laminae (Fig. 1D).

Optimisations for stable cellular imaging

A critical issue was to achieve sufficient stability for high-resolution measurements of cellular Ca²⁺ dynamics. Prior to stabilisation we observed sliding movements of the SC along the rostral-caudal body axis clearly associated with breathing (Supplementary Movie 1). These macroscopic movements could be minimised by

attaching vertebral clamps (Fig. 1A) and by slightly elevating the mouse to mechanically isolate the SC from respiratory movements (Davalos *et al.* 2008) (Supplementary Movie 2). Animal posture was further optimized with a mouse tooth bar to maintain an elongated neck region. Together with keeping the upper airways free of mucus this approach resulted in smooth breathing throughout the experiment.

Despite these measures rhythmic movements in the 1–2 Hz frequency range often remained at the microscopic level impeding functional two-photon imaging of DH cells within a focal plane (Supplementary Movie 3). The motion artefacts in fluorescence signals from cellular regions of interest were significantly reduced, however, by applying agar and a coverglass to the exposed SC (Fig. 2A and B; Supplementary Movie 4; amplitude of baseline fluctuations $34 \pm 0.9\% \Delta F/F$ before and $5.3 \pm 0.2\% \Delta F/F$ after stabilization; $n = 46$ cells from 4 animals; $P < 0.001$, t test). Thus, baseline noise levels could be sufficiently lowered to enable monitoring of fast Ca²⁺ transients in single DH neurons for several hours.

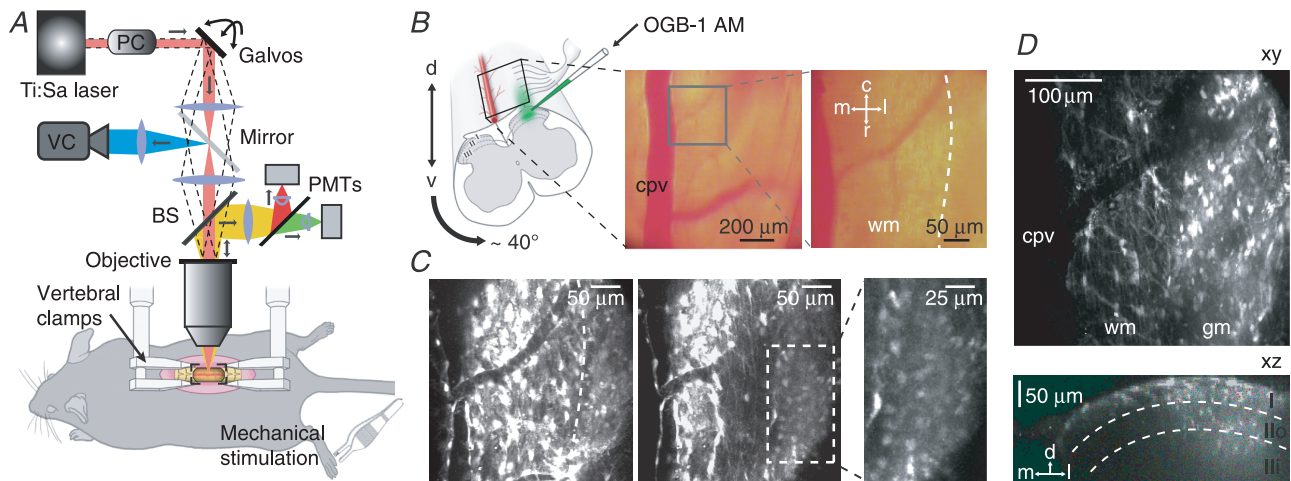


Figure 1. Set-up for two-photon Ca²⁺ imaging in the mouse dorsal horn

A, schematic diagram of the mouse preparation and the two-photon microscope set-up. The mouse was fixed in a stereotactic frame by attaching custom-made clamps to the vertebral column. A Ti:sapphire laser was used for two-photon excitation of fluorescence and galvanometric scan mirrors to deflect the laser beam. Laser intensity was adjusted with a Pockels cell (PC). Fluorescence was detected with photomultiplier tubes (PMTs). A video camera (VC) was used to visualize blood vessels and guide pipettes for staining and stimulation procedures. Switching between two-photon and video mode was accomplished by sliding the beamsplitter (BS) out of the beam path and sliding in an extra mirror (grey). B, the animal was rotated by approximately 40 deg around its longitudinal axis to obtain an approximately perpendicular surface and to optimize optical access to the lateral grey matter. Two video images of the SC surface are shown at different zoom level. The prominent central posterior vessel (cpv) located at the spinal midline and its branches served as landmarks for OGB-1 injection. Dashed white curve delineates the lateral white matter (wm) border. d: dorsal; v: ventral; m: medial; l: lateral; r: rostral; c: caudal. C, two-photon fluorescence images of the same field of view as in the right image in B after OGB-1 loading, exemplifying the typical staining patterns at different depths (left: about 30 μm ; middle: about 70 μm). Right: zoom-in of the middle image showing the faintly OGB-1-labelled population of DH cells. D, example images of OGB-1-staining from a different experiment. Top view (xy): maximum intensity projection at 50–100 μm depth; labelled cell populations were preferentially found in the lateral field, representing superficial grey matter (gm). Side view (xz): labelled SC cells could be imaged down to about 200 μm depth. Note the spinal cords' inherent bending; white dashed lines indicate lamina borders, laminae are indicated in Roman numerals.

Spontaneous and evoked Ca^{2+} transients in SDH neurons

In approximately 5% of SDH cells we observed spontaneous Ca^{2+} transients characterized by a sharp initial rise followed by a slower decay (Fig. 2C) which is indicative of action-potential evoked neuronal Ca^{2+} transients (Stosiek *et al.* 2003). The decay often could be approximated with an exponential function. Spontaneous events had mean peak amplitudes of $17.2 \pm 1.2\%$ $\Delta F/F$ and a mean decay time constant of 0.80 ± 0.09 s ($n = 24$ cells from 4 animals). Additionally,

slow spontaneous Ca^{2+} -oscillations of about 20% $\Delta F/F$ amplitude and several seconds duration were observed in some of the brightly labelled SDH cells, presumably representing slow glial calcium signals (Fig. 2D). Upon electrical stimulation of primary afferent fibres we typically found that a larger fraction of OGB-1-positive cells was activated in a stimulus intensity-dependent manner (Fig. 2E). With increasing stimulus strength previously silent cells became active at a certain threshold, showing responses of increasing amplitude (Fig. 2F). The fraction of active cells ranged from about 10% at

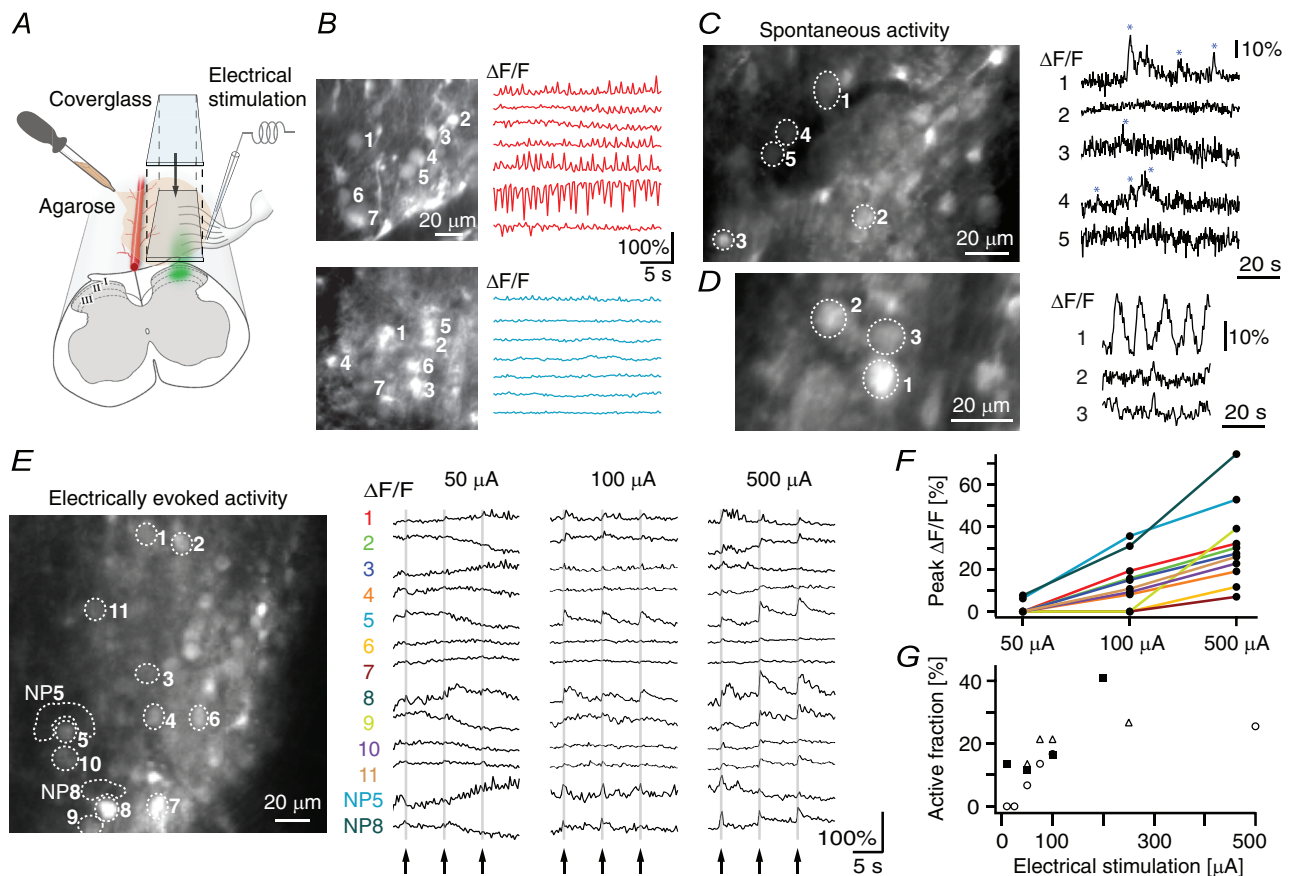


Figure 2. Spontaneous and evoked signals in the stabilized SC

A, schematic diagram showing SC stabilisation by applying a layer of agarose at body temperature to the dorsal SC surface above the OGB-1-labelled region and placing a coverglass carefully on top. For electrical stimulation, a glass pipette was inserted into primary afferent fibres projecting into the labelled area. B, two-photon images showing OGB-1-stained SC neuronal populations at about 50 μm depth. The fluorescence traces were obtained from regions of interests corresponding to the cells indicated by white numerals to their right (descending order of traces from top to bottom). Red traces in the top example show large motion artefacts before tissue stabilization; blue traces in the lower example were obtained in the same animal after stabilization. C, two-photon image of OGB-1-labelled SDH cells. Several fluorescence traces from the marked example cells display spontaneous Ca^{2+} transients (blue asterisks). D, image of OGB-1-labelled SDH cells from a different experiment. Slow spontaneous Ca^{2+} oscillations occur in a presumed glia cell (no. 1) displaying a high baseline fluorescence. E, field of view, in which electrical activation of primary afferents evoked Ca^{2+} transients. Electrically evoked fluorescence changes are shown in the marked subpopulation for three consecutive stimulations with a short pulse train (arrows) at three different stimulation strengths. F, peak amplitude of fluorescence transients from the same set of cells (colour-coded according to numbers in E) plotted for three stimulation strengths. G, the fraction of cells that showed stimulus-evoked responses as a function of stimulus strength. Data points from three individual experiments are indicated by different marker symbols.

10–50 μA stimulus intensity to about 30% at >200 μA (Fig. 2G). Electrically evoked fluorescence transients displayed a fast initial rise and a mean decay time of 1.1 ± 0.05 s ($n = 44$ cells from 4 animals). We conclude that action-potential evoked Ca²⁺ transients are triggered in SDH cells by electrical stimulation of afferent fibres and can be readily resolved by *in vivo* two-photon imaging.

Pinch-evoked Ca²⁺ transients in SDH neurons

Finally we measured activation of SDH cells following sensory stimulation. Mechanical stimulation of the ipsilateral hindpaw with a pinch device elicited Ca²⁺ transients in approximately 10% of OGB-1-stained cells within the field of view (Fig. 3A and B). Sensory-evoked Ca²⁺ transients had a mean amplitude of $13.3 \pm 0.7\%$ $\Delta F/F$ and a mean decay time constant of 0.77 ± 0.08 s (Fig. 3C and D; $n = 25$ cells from 5 animals). We conclude that the above described optimizations of experimental conditions make it possible to resolve sensory-evoked Ca²⁺ transients in SDH neurons, presumably resulting from synaptically driven generation of one or a few action potentials.

Discussion

Most *in vivo* imaging studies of mouse SC have focused on morphological changes of neurons and glial cells over the time course of hours to weeks, benefiting in particular from mouse lines with genetically labelled cell populations (Kerschensteiner *et al.* 2005; Davalos *et al.* 2008; Dray *et al.* 2009). Here, we have advanced functional imaging of fast neural activity in the SDH of living mice using two-photon microscopy. In contrast to population Ca²⁺ imaging in brain areas, motion artefacts – primarily induced by breathing-related tissue movements – constitute a major problem for SC imaging in living animals. Previous studies employed various methods to stabilise the SC including vertebral clamping, pneumothorax and artificial ventilation (Furue *et al.* 1999; Bester *et al.* 2000; Sasaki *et al.* 2002; Kerschensteiner *et al.* 2005; Ikeda *et al.* 2006; Davalos *et al.* 2008; Drdla *et al.* 2009). Here, we succeeded in achieving stable high-resolution imaging in freely breathing mice by optimizing mechanical stabilization of the vertebral column and animal posture, and by dampening local tissue pulsations with agar. These optimizations were critical for measuring spontaneous and evoked Ca²⁺ transients in SDH cells on a fast time scale.

Previous optical studies of SC function suffered from either limited spatial (Sasaki *et al.* 2002) or limited temporal (Ikeda *et al.* 2006; Drdla *et al.* 2009) resolution. Here, we report optical detection of fast Ca²⁺ transients in SDH cell populations at cellular resolution. For SC

imaging, a comparable spatiotemporal resolution has been so far achieved only for zebrafish larvae (Brustein *et al.* 2003). Even though it is unclear whether the sensitivity of our two-photon measurements currently is sufficient to resolve Ca²⁺ transients evoked by single action potentials, our finding of sparse spontaneous activity in SDH agrees well with several electrophysiological studies using single-cell recordings in anaesthetized rodent preparations (Furue *et al.* 1999; Bester *et al.* 2000; Graham *et al.* 2004). In particular, these studies also report pinch-evoked action

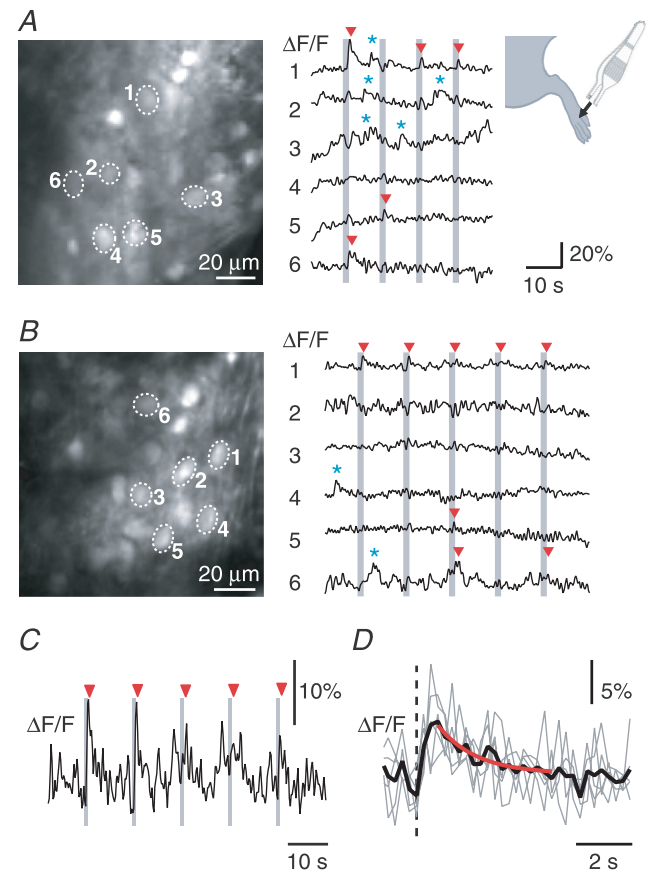


Figure 3. Pinch-evoked Ca²⁺ transients in a subset of SDH neurons *in vivo*

A, two-photon image showing an OGB-1-stained neuronal population approximately 50 μm from the pial surface including cells activated by pinch stimulation (vertical grey bars; schematic diagram to the right illustrates the mechanical stimulation applied to the ipsilateral hindpaw). Fluorescence traces from the marked example cells show stimulus-locked signal increases (red triangles). Additional spontaneous Ca²⁺ transients were not tightly locked to the stimuli (blue asterisks). B, two-photon image of another OGB-1-labelled SDH population from a different experiment acquired at about 70 μm depth. Example fluorescence traces are presented in the same way and on the same scales as in A. C, magnified fluorescence signal trace corresponding to cell 1 in panel B. Vertical grey bars indicate repeated pinch stimulation, red triangles mark evoked responses. D, average time course of the pinch-evoked Ca²⁺ transients shown in C (black trace) and exponential fit to the decay (red trace); individual Ca²⁺ transients aligned to stimulation onset (dashed line) are shown in light grey.

potential firing in subsets of SDH neurons, which seems to be a likely source of the response patterns we detect optically using similar stimulation protocols.

Functional studies of SC dorsal horn using two-photon Ca^{2+} imaging can be extended in the future in several ways. First, emerging advances in large-scale and high-speed population imaging (Grewe & Helmchen, 2009) will help to obtain a comprehensive picture of SDH activity *in vivo*. Second, cell type-specific counterstaining will be essential to dissect the SDH circuitry. Despite a preference for staining glia-like cells, SR101 does not seem to be a fully specific marker for astrocytes in the SC as opposed to the neocortex (Nimmerjahn *et al.* 2004). In future applications of our approach, transgenic mouse lines with selective labels as well as retrograde tracing techniques will thus be useful with respect to live discrimination of SC cellular subpopulations. Third, expression of genetically encoded Ca^{2+} indicators (Lütcke *et al.* 2010) might enable repeated functional imaging over days. This could be particularly beneficial to further studying cellular mechanisms of plasticity and pathophysiology in pain models or following experimental SC injury. Thus, high resolution imaging approaches as presented here can be expected to provide functional population data and new perspectives that will significantly advance our understanding of SC function and pathophysiology *in vivo*.

References

- Bester H, Chapman V, Besson JM & Bernard JF (2000). Physiological properties of the lamina I spinoparabrachial neurons in the rat. *J Neurophysiol* **83**, 2239–2259.
- Brusteine E, Marandi N, Kovalchuk Y, Drapeau P & Konnerth A (2003). “In vivo” monitoring of neuronal network activity in zebrafish by two-photon Ca^{2+} imaging. *Pflugers Arch* **446**, 766–773.
- Davalos D, Lee JK, Smith WB, Brinkman B, Ellisman MH, Zheng B & Akassoglou K (2008). Stable in vivo imaging of densely populated glia, axons and blood vessels in the mouse spinal cord using two-photon microscopy. *J Neurosci Methods* **169**, 1–7.
- Dray C, Rougon G & Debarbieux F (2009). Quantitative analysis by in vivo imaging of the dynamics of vascular and axonal networks in injured mouse spinal cord. *Proc Natl Acad Sci U S A* **106**, 9459–9464.
- Drdla R, Gassner M, Gingl E & Sandkuhler J (2009). Induction of synaptic long-term potentiation after opioid withdrawal. *Science* **325**, 207–210.
- Furue H, Narikawa K, Kumamoto E & Yoshimura M (1999). Responsiveness of rat substantia gelatinosa neurones to mechanical but not thermal stimuli revealed by in vivo patch-clamp recording. *J Physiol* **521**, 529–535.
- Graham BA, Brichta AM & Callister RJ (2004). In vivo responses of mouse superficial dorsal horn neurones to both current injection and peripheral cutaneous stimulation. *J Physiol* **561**, 749–763.
- Grewe BF & Helmchen F (2009). Optical probing of neuronal ensemble activity. *Curr Opin Neurobiol* **19**, 520–529.
- Ikeda H, Stark J, Fischer H, Wagner M, Drdla R, Jager T & Sandkuhler J (2006). Synaptic amplifier of inflammatory pain in the spinal dorsal horn. *Science* **312**, 1659–1662.
- Kerschensteiner M, Schwab ME, Lichtman JW & Misgeld T (2005). In vivo imaging of axonal degeneration and regeneration in the injured spinal cord. *Nat Med* **11**, 572–577.
- Lütcke H, Murayama M, Hahn T, Margolis DJ, Astori S, Meyer zum Alten Borgloh S, Göbel W, Yang Y, Tang W, Kügler S, Sprengel R, Nagai T, Miyawaki A, Larkum ME, Helmchen F & Hasan MT (2010). Optical recording of neuronal activity with a genetically-encoded calcium indicator in anesthetized and freely moving mice. *Frontiers in Neural Circuits* **4**, 9.
- Nimmerjahn A, Kirchhoff F, Kerr JN & Helmchen F (2004). Sulforhodamine 101 as a specific marker of astroglia in the neocortex in vivo. *Nat Methods* **1**, 31–37.
- Sasaki S, Yazawa I, Miyakawa N, Mochida H, Shinomiya K, Kamino K, Momose-Sato Y & Sato K (2002). Optical imaging of intrinsic signals induced by peripheral nerve stimulation in the in vivo rat spinal cord. *Neuroimage* **17**, 1240–1255.
- Steffens H, Nadrigny F, Dibaj P, Neusch C, Schomburg ED & Kirchhoff F (2009). Preparations of the mouse spinal cord for in vivo imaging by 2-photon laser-scanning microscopy. Abstract T27–2A in *Proceedings of the 8th Meeting of the German Neuroscience Society 2009*.
- Stosiek C, Garaschuk O, Holthoff K & Konnerth A (2003). In vivo two-photon calcium imaging of neuronal networks. *Proc Natl Acad Sci U S A* **100**, 7319–7324.
- Willis WD Jr (2007). The somatosensory system, with emphasis on structures important for pain. *Brain Res Rev* **55**, 297–313.

Author contributions

H.C.J. and F.H. conceived and designed experimental procedures; H.C.J. performed all experiments; H.C.J. and F.H. analysed the data and wrote the manuscript. All authors approved the final version of the manuscript for publication.

Acknowledgements

We thank Heinz Steffens and Frank Kirchhoff for help with the spinal cord preparation, Björn Kampa and Benjamin Grewe for discussions, Hansjörg Kasper, Stefan Giger, Martin Wieckhorst, Roland Schöb, Caroline Aemisegger and Eva Hochreutener for excellent technical assistance and David Margolis for critical revision of the manuscript. This work was supported by the National Centre of Competence in Research ‘Neural Plasticity and Repair’, the Neuroscience Centre Zurich, the Swiss National Science Foundation (Grant 3100A0-114624), and the EC-FP7 project Plasticise (contract 223524).